RSC Advances

PAPER

Development and characterisation of switchable polyaniline-functionalised flow-through capillary monoliths†

Cite this: DOI: 10.1039/c4ra05565a

Patrick Floris,[a] Damian Connolly,[b] Blanaid White[a] and Aoife Morrin*[a]

Received 10th June 2014
Accepted 1st September 2014

DOI: 10.1039/c4ra05565a

www.rsc.org/advances

Polymer monoliths were prepared in capillary format (250 μm i.d.) and used as solid supports for the immobilisation of the conducting polymer polyaniline (PANI). The immobilisation of PANI was confirmed on the large macro-porous structure of a polystyrene–divinylbenzene (PS-*co*-DVB) monolith. The surface coverage of polyaniline was characterised by field emission scanning electron microscopy (FE-SEM) and by capacitively coupled contactless conductivity detection (C^4D), which was operated in scanning mode to non-invasively visualise the axial distribution of the immobilised PANI and to provide information on its doping state. To further demonstrate the successful functionalisation of the monoliths, the PANI-functionalised monoliths were demonstrated as switchable, weak anion-exchange stationary phases as confirmed by studying the retention of iodide using a perchlorate eluent.

Introduction

Conductive organic polymers (CPs) have been the subject of great research interest over the last 30 years.[1,2] These materials undergo dramatic rapid and reversible physico-chemical changes by the application of a stimulus. Specifically, pH and redox switching of CPs can be accompanied by dramatic changes in properties such as the hydrophobicity and ion-exchange capacity.[3,4] Among conducting polymers, polyaniline (PANI) in particular has been studied extensively and been successfully applied in many areas including the development of stimuli-responsive controlled drug release systems[5] and sensors.[6,7] The stimuli-responsive nature of PANI has also found application in separation science.[8] The preparation of a PANI-functionalised stationary phase was originally reported by Chriswanto *et al.* Silica particles (10 μm in diameter) were functionalised with PANI and packed in stainless steel housings (4.9 mm × 10 cm), with the chromatographic properties of the stationary phases evaluated in reversed-phase and ion-exchange modes using a series of standard test compounds (polycyclic aromatic hydrocarbons and small ions). Applications in capillary electrophoresis (CE) have also been reported by Bossi *et al.*[10] who modified the inner walls of fused-silica capillaries with thin layers of PANI for the separation of peptides. The mechanism of separation in this instance was related to the hydrophobic–hydrophobic interaction between the peptides and PANI coatings.

Various electrochemical and chemical syntheses of PANI with a range of resulting morphologies (rods, fibres and spherical particles) have been reported.[11] Compared to thick bulk polyaniline films, PANI thin films (<100 nm) results in faster response times and reduced penetration depths for target analytes[12] due to the enhanced surface to volume ratio typical of nano materials.

The majority of methods employed for the growth of PANI films on solid substrates are based upon the polymerisation of aniline under acidic conditions using a persulfate oxidant.[13] For example Ince *et al.*[14] described the functionalisation of polystyrene (PS) microspheres with PANI for cellulase immobilisation using a two-step approach which involved the electrostatic attachment of aniline on the sulphonated PS surface followed by immersion of the aniline-functionalised spheres in a potassium persulfate solution. This lead to the formation of thick PANI layers (16 μm average depth). Core–shell poly(methyl methacrylate) (PMMA) particles coated with PANI have also been reported.[15] A 0.55 μm layer of PANI was formed on the surface of the PMMA cores upon treatment with ethylene glycol dimethacrylate, glycidyl methacrylate and oxydianiline which were used as cross-linking, grafting and swelling agents respectively.

Alternative supports for PANI are monolithic polymer materials which are single, continuous pieces of polymer. They have been used extensively in chromatography over the last 20 years[16,17] because of the high inter-pore connectivity which allows efficient separations to be achieved at high flow rates due to the low pressure-drop across the column. Continuous porous

[a]School of Chemical Sciences, National Centre for Sensor Research, Dublin City University, Dublin 9, Ireland. E-mail: aoife.morrin@dcu.ie; Fax: +353 1 700 5503; Tel: +353 1 700 6730

[b]Pharmaceutical and Molecular Biotechnology Research Centre (PMBRC), Department of Chemical and Life Sciences, Waterford Institute of Technology, Waterford, Ireland

† Electronic supplementary information (ESI) available. See DOI: 10.1039/c4ra05565a

PANI monoliths have been prepared in microfluidic housings as recently described by Gorey *et al.*[18] who demonstrated the fabrication of an inverse-opal conducting PANI monolith *via* electrochemical growth of PANI within the interstices of a sacrificial PS colloidal crystal template. The monolith's mechanical stability and bonding with the channel walls however, was not fully explored. A more mechanically robust monolith could potentially be prepared by blending PANI with conventional methacrylate- or styrene-based polymers.[19] However it is anticipated that this could hinder the electrochemically switchable properties of PANI. For this reason, the immobilisation of a thin film of PANI on an existing monolithic solid support represents a more attractive option in order to counteract this limitation. It also allows the morphology and flow-through properties of the underlying monolith to be easily optimised, independently of a subsequent PANI coating step.

Modifying monoliths with homogeneous thin films of PANI potentially provides an ideal format for studying stimuli-responsive chromatography using conducting polymers. This work builds on that of Wallace in the early 90's where he attempted to study the chromatographic behaviour of these materials on particulate packings.[8,20] However the challenge at this time was that in order to create an electrically conducting stationary phase (for use in electrochemically modulated liquid chromatography (EMLC)), particles must be in contact both with each other and with the column walls. This is clearly not the case with particulate stationary phases due to the presence of interstitial voids but could be overcome by moving from a particulate to a continuous support, as described here.

The characterisation of monolithic stationary phases and coatings to date has mainly involved the use of invasive techniques such as FE-SEM or energy-dispersive X-ray spectroscopy (EDX). These techniques are very useful for obtaining visual and qualitative information on the monolith's properties but are only representative of a specific region of the monolith itself and require the sample to be dry. Hence, they do not provide direct information under operational conditions. Recently sC^4D has emerged as a useful characterisation tool for monolithic stationary phases,[21] especially in capillary format, due to its ability to provide information about stationary phase properties in a completely non-invasive manner. Some recent applications include the evaluation of surfactant coatings on capillary monoliths,[22] the verification of structural homogeneity of monolithic rods[23] and the visualisation of charged functionalities along monolithic surfaces.[24] One distinct aspect of this technique is that the detection is "contactless" since the signal, which is passed through the bore of two ring electrodes placed at a fixed distance apart, is capacitively coupled through the walls of insulating tubing (such as fused silica capillaries).

In the work described here, thermoplastic polymer monoliths were prepared in capillary format (250 μm i.d.) and coated with thin films of PANI. The surface coverage of PANI was visualised by FE-SEM. sC^4D was used to non-invasively determine the distribution of PANI along the surface. The switching of PANI from its neutral emeraldine base to charged salt was also indirectly visualised using sC^4D. Ion-exchange properties of these stationary phases were also demonstrated, illustrating the potential of these materials as chromatographic stationary phases.

Experimental methods

Materials and reagents

Aniline (purified by distillation), hydrochloric acid (HCl), nitric acid (HNO_3), sodium hydroxide (NaOH), ammonium persulphate, polystyrene, divinylbenzene, 1-propanol, 1,4-butanediol, butyl methacrylate (BuMA), ethylene glycol dimethacrylate (EDMA), lauryl methacrylate (LMA), aminoethyl methacrylate hydrochloride (AEMA), azobisisobutyronitrile (AIBN), dodecanol, DMF, potassium bromide, potassium perchlorate and potassium iodide were purchased from Sigma Aldrich (Dublin, Ireland). Polyimide coated fused silica capillary (250 μm i.d.) was purchased from Composite Metal Services (Shipley, UK).

Instrumentation

A TraceDec capacitively coupled contactless conductivity detector (Innovative Sensor Technologies GmbH, Innsbruck, Austria) was used for sC^4D measurements. A Knauer K120 pump (Knauer, Berlin, Germany) was used for performing all monolith flushing/equilibration steps and during the acquisition of sC^4D profiles. A GFL water bath (MSC Medical Supply, Dublin, Ireland) was used for the preparation of polymer monoliths and FE-SEM analysis was performed using a Hitachi S-5500 FE-SEM instrument (Hitachi, Maidenhead, UK). Ion-exchange separations were performed using a Dionex Ultimate 3000 capillary LC system equipped with a 45 nL UV flow cell (Sunnyvale, CA, USA). A Parkin Elmer Spectrum 100 FT-IR (San Jose, CA, USA) was used for IR analysis of the PANI-modified polymer monoliths.

Fabrication of polymer monoliths

Three methacrylate monoliths of varying hydrophobicity were prepared along with three polystyrene–divinylbenzene (PS-*co*-DVB) monoliths as summarised in Table 1 below and described in the ESI.†

Modification of monoliths with PANI films

A solution containing 15 μL mL^{-1} of aniline and 9 mg mL^{-1} ammonium persulphate in 1 M HCl was pumped through the monoliths *via* syringe for 30 s in one direction, followed by 30 s in the reverse direction. The monoliths were then sealed at both ends using rubber septa and left standing at room temperature for 30 min, followed by a rinse with water at 3 μL min^{-1} for 5 min. The entire PANI coating process was carried out once for the methacrylate monoliths, but was repeated 3 times for each of the PS-*co*-DVB monoliths.

Evaluation of axial homogeneity of PANI coatings using sC^4D

Scanning contactless conductivity detection was used to evaluate the axial homogeneity of PANI coverage along the length of all monoliths using methods previously described by Connolly *et al.*[21] and described in detail in the ESI.†

Table 1 Summary of polymer monoliths prepared for modification with PANI

	AEMA (wt%)	BuMA (wt%)	LMA (wt%)	PS (wt%)	DVB (wt%)	EDMA (wt%)	1-Propanol (wt%)	1,4-Butanediol (wt%)	Dodecanol (wt%)	DMF (wt%)
AEMA[a]	24	—	—	—	—	16	—	—	30	30
BuMA[a]	—	24	—	—	—	16	35	25	—	—
LMA[a]	—	—	24	—	—	16	40	20	—	—
PS[a]	—	—	—	20	20	—	—	—	60	—

[a] All monoliths contained 1 wt% AIBN w.r.t. monomer.

Indirect verification of doping state of immobilised PANI using sC^{4}D

Bare unmodified PS-*co*-DVB monoliths were initially characterised using sC^{4}D while pumping deionised water at 3 μL min^{-1} using the following detector conditions: frequency 2× high, input voltage 0 dB and offset 000. After modification with a single PANI coating as described, the monolith was first equilibrated overnight (~15 h) with 1 M NaOH at 1 μL min^{-1} and then water at 3 μL min^{-1} for 6 h prior to sC^{4}D profiling using the same detector settings.

A sC^{4}D profile of the column under acidic conditions was also obtained. The same column was equilibrated for 6 h in 1 mM HNO_3 at 3 μL min^{-1} prior to obtaining readings using the following detector settings: frequency 2× high, input voltage −24 dB and offset 000. A 1 M HCl solution was then flushed overnight at 1 μL min^{-1} to facilitate protonation of the immobilised PANI. Finally conductivity responses were measured after equilibrating the column in 1 mM HNO_3 for 6 h at 3 μL min^{-1}.

Determination of ion-exchange properties

A PS-*co*-DVB monolith, which was modified 3 times with PANI, was used to evaluate the ion-exchange properties of the stationary phase. Retention of 1 mM iodide was observed under identical detection conditions after injecting 100 nL volumes of iodide, using a 0.1 mM perchlorate eluent at a flow rate of 10 μL min^{-1}. The de-doping of the column was achieved by pumping 1 M NaOH overnight at 1 μL min^{-1} followed by a rinse in deionised water for 1 hour at 3 μL min^{-1}. The ion-exchange capacity was also determined as described in the ESI.†

Results and discussion

Preparation of monolithic supports

The synthesis of conductive blends of PANI with PMMA[19] and PS[25] has been previously reported however, the absence of flow-through pores in the resulting materials restricts their applicability in the separation science sphere. Therefore, the feasibility of modifying an existing polymer monolith with a coating (or multiple coatings) of PANI was explored in this work. It was anticipated that the successful adsorption of PANI (a relatively hydrophobic polymer) onto the monolith surface would be dependant to a certain extent upon the relative hydrophobicity of the monolith. For this reason, a number of methacrylate monoliths were prepared in which the functional monomer was increasingly hydrophobic (from AEMA to BuMA to LMA) while using the same crosslinker (EDMA). In all cases the monomer/crosslinker ratio was held constant as was the total monomer/porogen ratio. However as shown in Table 1, the nature of the porogen system varied between each methacrylate monolith due to solubility differences between each functional monomer.

It is well known that the nature of both the porogen system and the functional monomer has a significant effect upon monolith pore size[26] and so the monolith morphology of each methacrylate monolith was expected to be significantly different from each other. FE-SEM images illustrating the different macro-porous structures of each of the polymer monoliths is given in ESI-4.† Our primary goal however in this work was (a): to investigate the relationship between monolith hydrophobicity and PANI coating integrity and (b): to interrogate the switching properties of the resulting coatings. Therefore, differences in monolith morphology were not considered pertinent in this initial study; in each case the bare unmodified monoliths exhibited suitably low operating back pressures for the flow-through studies.

Functionalisation of monoliths with PANI

The oxidative polymerisation of aniline using ammonium persulphate as oxidant proceeds rapidly (<30 min) in bulk acidic solution. Therefore, the acidified aniline/persulphate solution was flushed through the monoliths without delay after preparation, such that the polymerisation of PANI occurred within the pore volume of the monoliths. As such, it was anticipated that a thin PANI film of controlled thickness would adsorb onto the monolith globules. The aniline/persulphate solution was flushed through the monolith in both directions in order to maximise the axial homogeneity of PANI coverage (based upon reports by Gillespie *et al.*[22] who observed unintentional inhomogeneity of surfactant coverage when silica-based C_{18} monoliths were coated with surfactants in one direction only).

The formation of PANI aggregates within the pore volume has potential to cause unintentional partial or total blockage of the monolith pores. Thus, FE-SEM imaging was used to evaluate both the integrity of the porous structure before and after PANI polymerisation, as well as the nature of the attachment of PANI to the monolith surface. The AEMA-*co*-EDMA monolith was intentionally selected as the most hydrophilic monolith in this

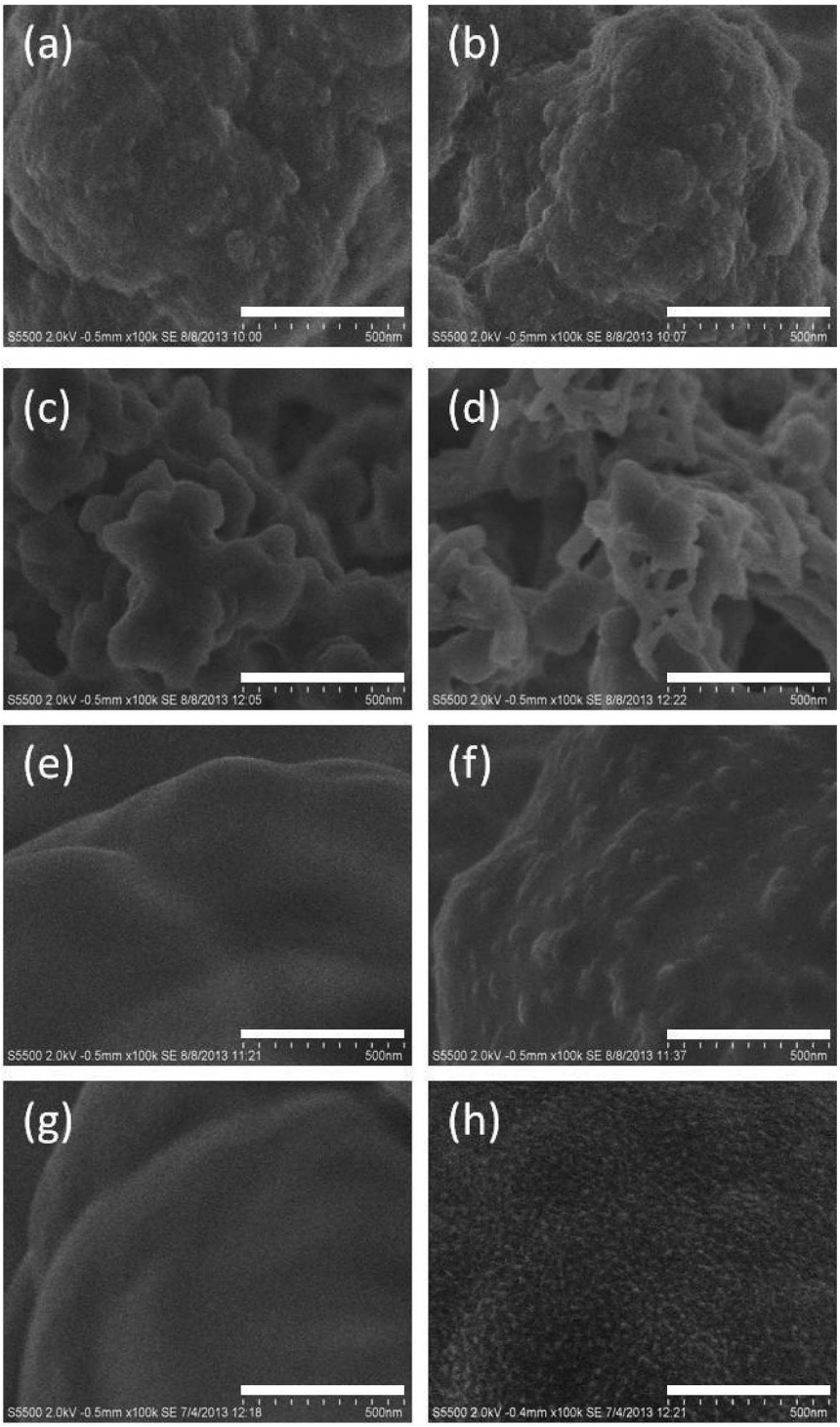

Fig. 1 FE-SEM images showing variations in surface morphology before (a, c, e and g) and after (b, d, f and h) modification with PANI. Comparison of (a and b) AEMA-*co*-EDMA, (c and d) BuMA-*co*-EDMA, (e and f) LMA-*co*-EDMA and (g and h) PS-*co*-DVB monoliths are illustrated (magnification: 100 000×).

study and as expected there was no discernable difference in surface roughness after the PANI modification step as shown in Fig. 1(a and b). Conversely, the BuMA-*co*-EDMA monolith resulted in a fibrillar-like mesh of PANI readily observable on the monolith surface, Fig. 1(c and d). The PANI structures appear not to be intimately bonded to the globule surface but instead appear physically entrapped within crevices between adjacent globules. Operating backpressure (pumping water at 3 μL min^{-1}) increased by 44% after PANI polymerisation, presumably due to partial pore blockage by large PANI

aggregates (Fig. 1(d)). Nevertheless, the retention of these PANI aggregates was tentatively attributed to the increased hydrophobicity of BuMA-*co*-EDMA relative to AEMA-*co*-EDMA. (It is presumed the weakly bound PANI was rapidly flushed from the AEMA-*co*-EDMA pore volume during subsequent monolith washing steps). For this reason, a LMA-*co*-EDMA monolith was employed as a substrate for comparative purposes since it was expected to lead to stronger hydrophobic attachment of PANI films due to its longer alkyl chain (C_{12}) relative to BuMA (C_4). Despite the greater hydrophobicity of LMA-*co*-EDMA monoliths, an unexpectedly patchy surface coverage of PANI was observed after functionalisation, as visualised in Fig. 1(e and f). Here PANI appeared as sparse individual nodules on an otherwise smooth surface. Nevertheless, this was considered a positive development as it was indicative of possible increased dispersive interactions between PANI and the C_{12} alkyl chain of LMA (along with dipole–dipole interactions given that the monolith was methacrylate based). Flow-through properties were not adversely affected for the PANI-coated LMA-*co*-EDMA monolith (with backpressures of 0.9 bar per cm at 3 μL min^{-1}).

In order to examine the effect of other interactions such as potential π–π interactions between the underlying monolith and PANI thin films, a PS-*co*-DVB monolith was prepared, again using a monomer/porogen composition which ensured a comparatively low operating backpressure.[26] Previous reports which describe the preparation of PANI-modified PS spheres involved an initial sulphonation of the PS in order to achieve a negatively charged surface which facilitated electrostatic binding of protonated aniline molecules prior to their polymerisation. Interestingly, prior sulphonation of the PS-*co*-DVB monolith was found to be unnecessary in this work, with the PANI formation step performed as per the methacrylate monoliths, thereby allowing a direct comparison of PANI coverage to be made.

Post-functionalisation of the PS-*co*-DVB monolith, a green colour along the entire monolith length was visible through the fused silica capillary housing. This was indicative of the emeraldine salt form of PANI and could readily be reversibly switched to a homogeneous violet colour (the emeraldine base form of PANI) by flushing the monolith overnight with 1 M NaOH as shown in Fig. ESI-2.† A marked improvement in PANI coverage over the methacrylate-based polymer monolith supports was observed (Fig. 1(g and h)) in which a PANI film with a nano-structured morphology evenly coats the PS-*co*-DVB monolith globules.

The modification process on the PS-*co*-DVB monolith was repeated up to 3 times which, as illustrated from the FE-SEM images shown in Fig. ESI-5,† lead to an apparent increase in the thickness of the PANI coating which appeared as an interconnected network with bud-like features. An small increase in operating backpressure from 0.2 to 0.3 bar per cm at a nominal flow of 3 μL min^{-1} was observed after modification with three coatings of PANI suggesting no dramatic change in flow-through properties of the monolith occurred. Further studies are required to determine the PANI coating thickness. The affinity of PANI for the monolith surface was attributed to both hydrophobic and π–π interactions between the benzene rings present in both aniline and the monolith backbone.[27,28] In this study, PS-*co*-DVB monoliths clearly represented the most ideal monolithic support for PANI adsorption given the coating homogeneity observed by FE-SEM.

Characterisation of PANI coverage using sC^4D

All monoliths were prepared in 250 μm i.d. fused silica capillaries since cross-sections of unmodified and PANI-modified monoliths could be easily prepared for subsequent FE-SEM analysis and also to facilitate facile sC^4D profiling experiments (which required 360 μm o.d. column housings due to the diameter of the ring electrodes within the commercial C^4D detector used in the work). In order to realise electrochemically modulated liquid chromatography (EMLC) with polymer monoliths, an electrochemical cell must be integrated into the capillary column. One approach to this could be employing the column housing itself as the working electrode. The integration of reference and auxiliary electrodes within the housing would also be required. Conducting column housings such as titanium or stainless steel could be considered as the working electrode component of the electrochemical cell under certain conditions. The group of Porter have established a viable column-based electrochemical cell for EMLC.[29,30] However, using conducting materials as capillary tubing prohibits the use of C^4D for characterisation purposes and so was not adopted for this work. We propose that such a format could potentially be employed in EMLC in future work to form the working electrode component of an electrochemical cell that could permit the electrochemical switching of the CP stationary phase *via* the application of a potential.

For a PANI-modified monolith to be useful for stimuli-responsive chromatography, the axial homogeneity of the PANI coating is critical; any gaps or fissures in the coating could impede its switching, *e.g.*, if the stimulus was electrical in nature and as such relied on a continuous film. Recently, reports illustrating the benefits of sC^4D for non-invasively characterising monolithic stationary phases in capillary formats have appeared in the literature. For this reason sC^4D was utilised in an effort to confirm the presence of PANI on the surface of the monoliths and potentially visualise pH switching of the chemical PANI state by way of this conductive response.

The conducting properties of PANI depend on its oxidation state and on the presence and nature of a dopant anion. Electron mobility is facilitated by the presence of a conjugated double bond structure which results in electron delocalization and facilitates the control of its conductive and insulating properties. It is known that under acidic conditions PANI is in a "doped" conductive state (the emeraldine salt form) with conductivity values that range from 10^{-2} to 100 S cm^{-1}. When exposed to strong bases however, PANI is reversibly converted to an insulating state (the emeraldine base form) and its conductivity decreases to values ranging from 10^{-10} to 10^{-7} S cm^{-1}.[31]

As illustrated in Fig. 2, the monoliths were subjected to sC^4D characterisation before and immediately after modification with PANI using a constant flow of 1 mM HNO_3 in order to dope the PANI coating. The scales of the detector responses in each

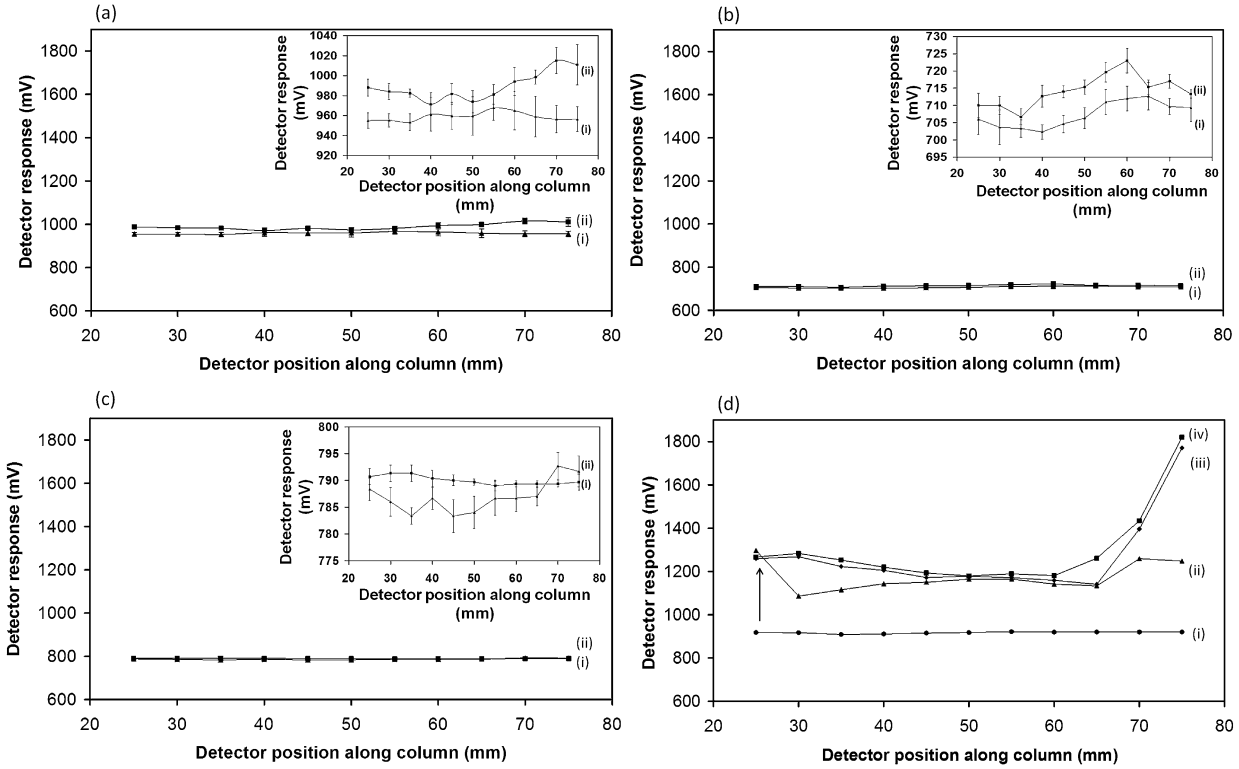

Fig. 2 sC^4D profiles in 1 mM HNO_3 (i) before and (ii) after modification with PANI of monoliths (a) AEMA-*co*-EDMA (b) BuMA-*co*-EDMA, (c) LMA-*co*-EDMA and (d) PS-*co*-DVB which was also modified a (iii) second and (iv) third time.

graph has been standardised in order to allow a comparison between conductive responses for each monolith upon modification with PANI. Profiles of monoliths AEMA, BuMA and LMA illustrated in Fig. 2(a–c) respectively, showed negligible changes in conductive response after modification with PANI (*e.g.* a maximum change of +60 mV for the AEMA monolith was observed). This is clearly visible from the zoomed-in conductive profiles of monoliths AEMA, BuMA and LMA shown as insets in Fig. 2(a–c) respectively. Conversely, a larger increase in conductive response (relative to the neutral uncoated monolith) was observed for the PS-*co*-DVB monolith in Fig. 2(d). The blank PS-*co*-DVB monolith displayed a homogeneous conductive response shown in Fig. 2(d)(i), indicating that no major defects in the monolith structure (*e.g.* localised areas of incomplete polymerisation) were present. Upon modification with PANI, shown in Fig. 2(d)(ii), sC^4D measurements revealed a 45% increase in conductive response. After a single modification, the presence of a non-homogeneous film was evident (most prominent in the initial 25–45 mm of column). After a second and third modification, shown in Fig. 2(d)(iii) and (iv) respectively, improved homogeneity in coverage was observed. The steep rise in conductivity observed after modification in the region between 65–75 mm of the column may be attributed to a localised pre-concentration effect during the functionalisation steps. This is visualised on one end of the column only since the initial 2 cm at the other end were covered by a connecting sleeve and hence remained uncharacterised. Two additional PS-*co*-DVB monoliths were subjected to the 3-step PANI coating process with sC^4D profiling also performed at each intermediate stage. The profiles in Fig. ESI-6† show that the PANI-coating procedure was repeatable on each monolith, with an increasing conductive response observed for each subsequent PANI coating, suggesting that the coating integrity improved after each PANI polymerisation step. Interestingly, sC^4D could be used in all cases to verify the presence of an inhomogeneity of coverage at the extremities of each monolith (which could easily be removed by cutting, before using the monoliths for subsequent chromatographic applications).

Verification of doping state of immobilised PANI using sC^4D

The use of sC^4D was also beneficial for obtaining information on the doped state of PANI immobilised on the surface of the PS-*co*-DVB monoliths. A PS-*co*-DVB monolith was initially characterised in deionised water as shown in Fig. 3(a)(i) and PANI was then immobilised on the surface. Upon flushing 1 M NaOH overnight, the monolith changed to a violet colour indicative of the emeraldine base form of PANI (Fig ESI-2†). Characterisation of this coating using sC^4D in water, shown in Fig. 3(a)(ii), revealed a very similar conductive response to the initial blank PS-*co*-DVB monolith indicating that the immobilised dedoped PANI did not contribute to an overall increase in conductive response.

The inset in Fig. 3(a) represents a zoomed-in view of the conductive profiles of the monolith before and after modification. Measurements were performed in triplicate and low standard deviation values were obtained (±5 mV) indicating the

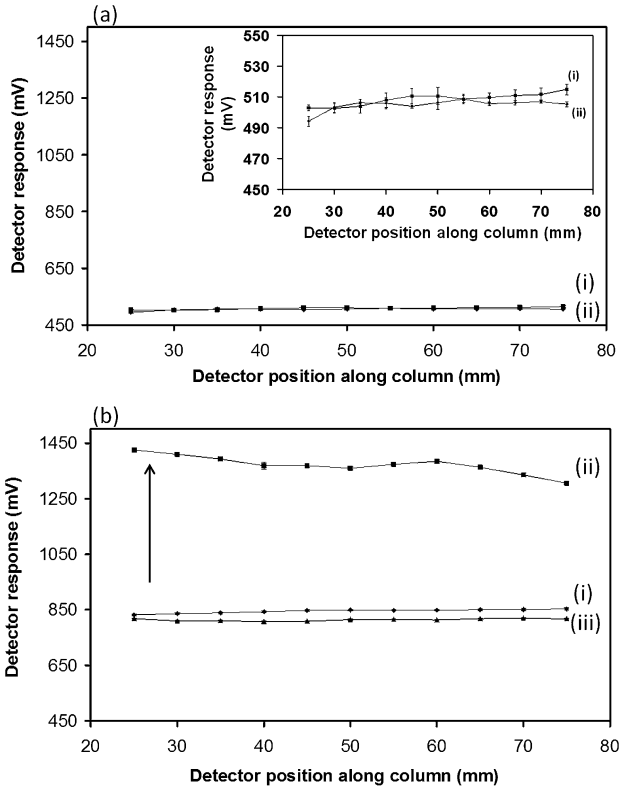

Fig. 3 (a) sC^4D profiles in water of a PS-*co*-DVB monolith (i) before and (ii) after modification with PANI followed by flushing the column in 1 M NaOH. (b) sC^4D profile of the same monolith in 1 mM HNO_3 illustrated in (a), (i) before and (ii) after protonation with 1 M HCl. A blank unmodified monolith (iii) is shown for comparative purposes.

reproducibility of the measurement. In a further step, the same column was characterised in 1 mM HNO_3, shown in Fig. 3(b)(i). It can be seen that under these conditions, full protonation of the immobilised PANI was not achieved. To enable complete protonation, 1 M HCl was flushed through the column to allow the switching of PANI into the emeraldine salt conductive form (observed as a green colour along the monolith length). This was confirmed again by obtaining sC^4D readings in 1 mM HNO_3, shown in Fig. 3(b)(ii), where a 70% increase in conductive response relative to the same column prior to protonation was observed. For comparative purposes, the sC^4D profile of an unmodified PS-*co*-DVB monolith, (Fig. 3(b)(iii)), was also included which had a similar profile to that obtained for the PANI-functionalised monolith in the dedoped (non-conducting) state.

Ion-exchange properties of the PANI-functionalised monolithic stationary phase

PANI coverage on the surface of the PS-*co*-DVB monolith was also confirmed by investigating its anion-exchange properties. A 13 cm long column was selected for this study which was adjusted to this length by removing the extremities of the functionalised monolithic capillary so as to have a homogeneous coverage of PANI as shown in Fig. 2(d). While bare PS-*co*-DVB monoliths are not suitable for performing as ion-exchange stationary phases, an ion-exchange capacity of 1.1 nano-equivalents per cm was observed upon modification with PANI due to the presence of protonated imine nitrogens. This value was calculated by flushing through the monolith the UV absorbing anion bromide which was then desorbed using a non-UV absorbing perchlorate eluent as described in ESI.†

Retention of iodide was also observed on the same column. Due to the low ion-exchange capacity of the stationary phase, a low ionic strength eluent which could also be an appropriate supporting electrolyte (0.1 mM perchlorate) was used.[32] Upon injection of a water blank, shown in Fig. 4(c), a void peak was visualised just before 5 min. After the injection of 1 mM iodide, shown in Fig. 4(a), a positive peak was visualised at 9.7 min which was indicative of the ion-exchange properties of the PANI-modified monolith. By flushing a 1 M solution of NaOH through the column in a further step, it was possible to de-dope the immobilised PANI. The absence of a peak at 9.7 min after the injection of iodide, shown in Fig. 4(b) confirmed that the PANI-coated monolith in the de-doped state no longer behaved as an ion-exchanger. The small ion-exchange capacity observed demonstrated that the emeraldine salt form of PANI was present on the surface of the PS-*co*-DVB monolith and could exchange its chloride dopant with ions in solution. The value

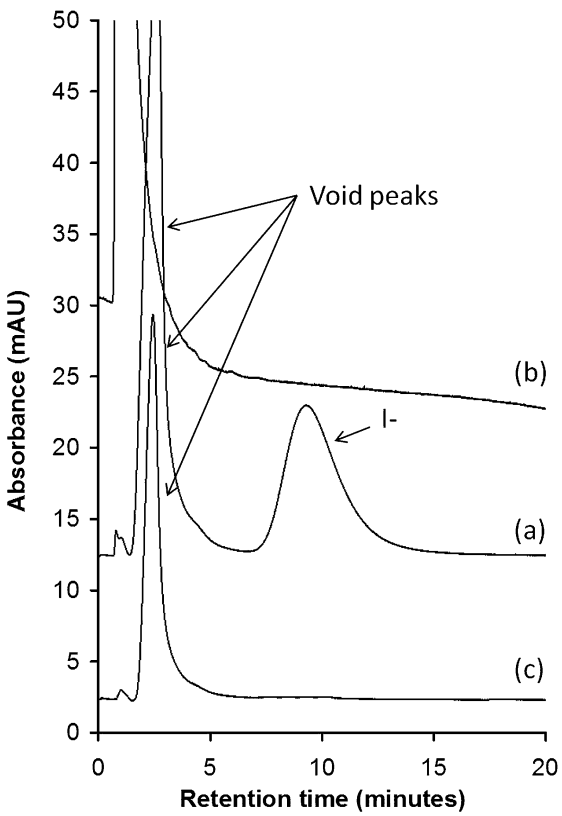

Fig. 4 Chromatograms obtained after the injection of iodide (1 mM) on a 13 cm long PANI functionalised PS-*co*-DVB monolith in doped (a) and dedoped (b) states. A water blank injection (c) is shown for comparative purposes. Eluent: 0.1 mM perchlorate. Flow rate: 10 μL min^{-1}. Detection: UV at 210 nm. Injection volume: 100 nL.

calculated however is low in comparison to previously reported ion-exchange monolithic stationary phases.[33] A possible explanation of this can be related to the deprotonation of imine nitrogens which occurred by flushing a non-acidic eluent such as perchlorate. Furthermore, the large macro-porous structure of the monoliths used here resulted in a very low surface area which would translate into limited chromatographic efficiency. Nonetheless the ion-exchange capacity of these materials has been demonstrated in principle.

Conclusions

In this work PANI-functionalised polymer monoliths were prepared in capillary format for the first time. The presence of strong π–π interactions between PANI and the PS-based monoliths resulted in a homogeneous surface coverage of PANI. The successful modification of the monoliths was confirmed by FE-SEM and sC^4D. This provided information on the axial distribution of the coating and on the doping state of the immobilised PANI. The use of these columns as switchable, weak ion-exchangers was also possible, as confirmed by the retention of iodide, demonstrating potential applications of these materials as chromatographic stationary phases. Current studies are ongoing to investigate control over hydrophobicity by varying the redox state and PANI dopants for reversed-phase applications. The porosity of the underlying monolith materials is also being investigated and optimised to improve the efficiency of these new PANI stationary phases. Its application in EMLC is also currently being investigated.

Acknowledgements

The authors would like to thank Science Foundation Ireland for funding under Grant no.: 12/TIDA/I2349.

Notes and references

1 C. Li, H. Bai and G. Shi, *Chem. Soc. Rev.*, 2009, **38**, 2397–2409.
2 J. Janata and M. Josowicz, *Nat. Mater.*, 2003, **2**, 19–24.
3 X. Y. Zhou, Z. Z. Zhang, X. H. Xu, X. H. Men and X. T. Zhu, *Appl. Surf. Sci.*, 2013, **276**, 571–577.
4 S. Taleb, T. Darmanin and F. Guittard, *RSC Adv.*, 2014, **4**, 3550–3555.
5 C. J. Perez-Martinez, T. del Castillo-Castro, M. M. Castillo-Ortega, D. E. Rodriguez-Felix, P. J. Herrera-Franco and V. M. Ovando-Medina, *Synth. Met.*, 2013, **184**, 41–47.
6 K. Crowley, M. R. Smyth, A. J. Killard and A. Morrin, *Chem. Pap.*, 2013, **67**, 771–780.
7 Y. Q. Hao, B. B. Zhou, F. B. Wang, J. Li, L. Deng and Y. N. Liu, *Biosens. Bioelectron.*, 2014, **52**, 422–426.
8 H. Ge and G. G. Wallace, *Anal. Chem.*, 1989, **61**, 2391–2394.
9 H. Chriswanto and G. G. Wallace, *Chromatographia*, 1996, **42**, 191–198.
10 A. Bossi, S. A. Piletsky, A. P. F. Turner and P. G. Righetti, *Electrophoresis*, 2002, **23**, 203–208.
11 D. Li and R. B. Kaner, *J. Am. Chem. Soc.*, 2006, **128**, 968–975.
12 R. Blair, H. Shepherd, T. Faltens, P. C. Haussmann, R. B. Kaner, S. H. Tolbert, J. Huang, S. Virji and B. H. Weiller, *J. Chem. Educ.*, 2008, **85**, 1102.
13 G. Z. Zhai, Q. Q. Fan, Y. Tang, Y. Zhang, D. Pan and Z. Y. Qin, *Thin Solid Films*, 2010, **519**, 169–173.
14 A. Ince, G. Bayramoglu, B. Karagoz, B. Altintas, N. Bicak and M. Y. Arica, *Chem. Eng. J.*, 2012, **189**, 404–412.
15 F. F. Fang, Y. D. Liu, I. S. Lee and H. J. Choi, *RSC Adv.*, 2011, **1**, 1026–1032.
16 G. Guiochon, *J. Chromatogr. A*, 2007, **1168**, 101–168.
17 F. Svec and C. G. Huber, *Anal. Chem.*, 2006, **78**, 2100–2107.
18 B. Gorey, J. Galineau, B. White, M. R. Smyth and A. Morrin, *Electroanalysis*, 2012, **24**, 1318–1323.
19 A. Fattoum, Z. Ben Othman and M. Arous, *Mater. Chem. Phys.*, 2012, **135**, 117–122.
20 H. Ge and G. G. Wallace, *J. Chromatogr.*, 1991, **588**, 25–31.
21 D. Connolly, P. Floris, P. N. Nesterenko and B. Paull, *TrAC, Trends Anal. Chem.*, 2010, **29**, 870–884.
22 E. Gillespie, D. Connolly, M. Macka, P. N. Nesterenko and B. Paull, *Analyst*, 2007, **132**, 1238–1245.
23 D. Connolly, V. O'Shea, P. Clark, B. O'Connor and B. Paull, *J. Sep. Sci.*, 2007, **30**, 3060–3068.
24 E. Gillespie, D. Connolly and B. Paull, *Analyst*, 2009, **134**, 1314–1321.
25 J. Bhadra, N. J. Al-Thani, N. K. Madi and M. A. Al-Maadeed, *Synth. Met.*, 2013, **181**, 27–36.
26 C. Viklund, F. Svec, J. M. J. Frechet and K. Irgum, *Chem. Mater.*, 1996, **8**, 744–750.
27 K. K. Sadasivuni, D. Ponnamma, P. Kasak, I. Krupa and S. A. A. Ali, *Mater. Chem. Phys.*, 2014, DOI: 10.1016/j.matchemphys.2014.06.055.
28 I. Brook, G. Mechrez, R. Y. Suckeveriene, R. Tchoudakov, S. Lupo and M. Narkis, *Polym. Compos.*, 2014, **35**, 788–794.
29 L. M. Ponton and M. D. Porter, *Anal. Chem.*, 2004, **76**, 5823–5828.
30 L. M. Ponton and M. D. Porter, *J. Chromatogr. A*, 2004, **1059**, 103–109.
31 M. J. R. Cardoso, M. F. S. Lima and D. M. Lenz, *Mater. Res.*, 2007, **10**, 425–429.
32 D. W. Keller, L. M. Ponton and M. D. Porter, *J. Chromatogr. A*, 2005, **1089**, 72–81.
33 J. P. Hutchinson, E. F. Hilder, R. A. Shellie, J. A. Smith and P. R. Haddad, *Analyst*, 2006, **131**, 215–221.